

Numerical bifurcation analysis of differential equations with state-dependent delay

T. Luzyanina, K. Engelborghs, D. Roose

Report TW 302, March 2000



Katholieke Universiteit Leuven
Department of Computer Science
Celestijnenlaan 200A – B-3001 Heverlee (Belgium)

Numerical bifurcation analysis of differential equations with state-dependent delay

*T. Luzyanina**, *K. Engelborghs*, *D. Roose*

Report TW 302, March 2000

Department of Computer Science, K.U.Leuven

Abstract

In this paper we extend existing numerical methods for bifurcation analysis of delay differential equations with constant delay towards equations with state-dependent delay. In particular, we study the computation, continuation and stability of steady state solutions and periodic solutions of such equations. We collect the relevant theory and point out open theoretical problems in the context of bifurcation analysis. We investigate two examples and compare computational results with analytical ones whenever possible. The results presented show that numerical bifurcation analysis of differential equations with state-dependent delay can be successfully achieved.

Keywords : delay equations, state-dependent delay, numerical bifurcation analysis.

AMS(MOS) Classification : Primary : 65J15, Secondary : 65P05.

*On leave from Institute of Mathematical Problems in Biology, RAS, Pushchino, Moscow region, 142292, Russia

1 Introduction

This paper deals with numerical bifurcation analysis of differential equations with *state-dependent* delay.

We concentrate on the following types of equations. First, consider

$$\begin{cases} \frac{d}{dt}x(t) = f_1(x(t), x(t - \tau(x(t)))) \\ \tau(x(t)) = g_1(x(t)), \end{cases} \quad (1)$$

where $f_1 : \mathbb{R}^n \times \mathbb{R}^n \rightarrow \mathbb{R}^n$, $g_1 : \mathbb{R}^n \rightarrow \mathbb{R}$, and the delay τ is a given (explicit) function of the solution $x(t)$. Note that explicit dependence of f_1 on τ as an argument is not necessary due to the explicit dependence of τ on x .

A second class of equations is given by

$$\begin{cases} \frac{d}{dt}x(t) = f_2(x(t), x(t - \tau(t)), \tau(t)) \\ \frac{d}{dt}\tau(t) = g_2(x(t), x(t - \tau(t)), \tau(t)), \end{cases} \quad (2)$$

where $f_2 : \mathbb{R}^n \times \mathbb{R}^n \times \mathbb{R} \rightarrow \mathbb{R}^n$, $g_2 : \mathbb{R}^n \times \mathbb{R}^n \times \mathbb{R} \rightarrow \mathbb{R}$, and the delay is determined by a differential equation.

We also consider threshold-type delay equations,

$$\begin{cases} \frac{d}{dt}x(t) = f_3(x(t), x(t - \tau(t)), \tau(t)) \\ \int_{t-\tau(t)}^t g_3(x(s))ds = 1, \end{cases} \quad (3)$$

where $f_3 : \mathbb{R}^n \times \mathbb{R}^n \times \mathbb{R} \rightarrow \mathbb{R}^n$, $g_3 : \mathbb{R}^n \rightarrow \mathbb{R}$, and the delay is determined implicitly by the solution segment through a *threshold condition*.

We assume that all functions in (1)-(3) are sufficiently smooth and that the delay is bounded, i.e., $0 \leq \tau(t) \leq r$, $\forall t$. In (1) the latter is assured by requiring $0 \leq g_1(x(t)) \leq r$, in (3) by requiring $g_3(x(t)) \geq 1/r > 0$.

Note that Eqs. (1)-(3) are connected in certain ways. Using $x_1 \equiv x$ and $x_2 \equiv \tau$, equation (2) can be considered as a particular case of (1) with the extended state $x \equiv (x_1, x_2)$. Also, differentiating the threshold condition in (3) with respect to t gives an equation of type (2) with

$$f_2 \equiv f_3, \quad g_2 \equiv 1 - \frac{g_3(x(t))}{g_3(x(t - \tau(t)))}. \quad (4)$$

Furthermore, equations (1) and (3) are particular cases of the class of equations,

$$\begin{cases} \frac{d}{dt}x(t) = f(x(t), x(t - \tau(t)), \tau(t)) \\ \int_{t-\tau(t)}^t g(x(t), x(s))ds = 1. \end{cases} \quad (5)$$

Indeed, when $g(u, v)$ is independent of v , the delay τ is determined by

$$\tau(x(t)) = (g(x(t)))^{-1}. \quad (6)$$

If $g(u, v)$ is independent of u , then the delay τ is determined by the integral condition,

$$\int_{t-\tau(t)}^t g(x(s)) ds = 1. \quad (7)$$

In the rest of this paper we explicitly deal with Eqs. (1)-(3). For notational convenience we restrict ourselves to a single delay, generalization to multiple delays is straightforward. We do not deal with Eq. (5) when $g(u, v)$ depends both on u and v . In this case bifurcation analysis involves distributed delays which are not under study in this paper.

Mathematical models with state-dependent delay are wide-spread in applications. For instance, a number of structured population models and models in epidemiology and immunology are specific cases of (5), see, e.g., [31, 32, 5] and the references therein. Recently mathematical models described by Eqs. (1)-(3) are proposed in [1, 7, 3, 25]. These applications show the necessity of a theory as well as numerical methods to analyze differential equations with state-dependent delay. Although important theoretical results were established, especially over the past several years, a number of open theoretical questions still exists due to the considerable complexity compared to the case of constant delays.

As far as we know, no prior work on the numerical study of the bifurcation behaviour of equations with state-dependent delay exists. Note that methods (see, e.g., [17, 33]) and software packages [30, 9] were developed for numerical time integration of Eq. (1). These packages can also deal with Eq. (2) by exploiting the above mentioned connection between (1) and (2).

Our aim here is to extend numerical methods for bifurcation analysis of differential equations with constant delay [24, 16, 14, 15, 11, 12] towards equations with state-dependent delay.

The remainder of this paper is structured as follows. In Sec. 2, we collect the relevant theoretical results and point out open problems in the context of bifurcation analysis. In Sec. 3 we show how numerical bifurcation analysis of Eqs. (1)-(3) can be achieved. Section 4 consists of examples which we study numerically in Sec. 5. Whenever possible we compare our numerical results with analytical ones, and we present bifurcation analysis of the equations under the conditions of and beyond restrictions posed by the existing theory. Section 6 contains some conclusions.

2 Theoretical Aspects

In this section we present theoretical results used in bifurcation analysis of differential equations with state-dependent delay (sd-DDEs).

2.1 Steady state solutions

A steady state solution of a sd-DDE is determined by the values of the solution x and the delay τ , i.e., the delay should be considered as a part of the state. Steady

state solutions, (x^*, τ^*) , of Eqs. (1)-(3) are solutions of

$$\begin{cases} f_1(x^*, x^*) = 0 \\ \tau^* = g_1(x^*), \end{cases} \quad (8)$$

respectively,

$$\begin{cases} f_2(x^*, x^*, \tau^*) = 0 \\ g_2(x^*, x^*, \tau^*) = 0 \end{cases} \quad (9)$$

and

$$\begin{cases} f_3(x^*, x^*, \tau^*) = 0 \\ \tau^* g_3(x^*) = 1. \end{cases} \quad (10)$$

The local stability of steady state solutions of sd-DDEs was studied in [8, 20]. It was shown, under natural assumptions on the right hand side of the equation and on the delay function τ , that generically the behaviour of the state-dependent delay τ except for its value τ^* has no effect on the stability, and that a local linearization is valid by treating τ as a constant at the steady state.

Hence to study the local stability of a steady state of (1), we linearize (1) at x^* by treating $\tau \equiv \tau^*$. The resulting linear equation is a *constant delay* differential equation,

$$\frac{d}{dt}y(t) = D_1 f_1(x^*, x^*)y(t) + D_2 f_1(x^*, x^*)y(t - \tau^*), \quad (11)$$

where (and below) $D_i h(s)$ denotes the partial derivative of the function $h(x_1, x_2, \dots)$ with respect to its i -th argument evaluated at s ,

$$D_i h(s) = \left. \frac{\partial h}{\partial x_i} \right|_s.$$

Similarly, for Eq. (2) stability of a steady state (x^*, τ^*) is analyzed through the linearization

$$\begin{cases} \frac{d}{dt}y_1(t) = D_1 f_2(x^*, x^*, \tau^*)y_1(t) + D_2 f_2(x^*, x^*, \tau^*)y_1(t - \tau^*) \\ \quad + D_3 f_2(x^*, x^*, \tau^*)y_2(t) \\ \frac{d}{dt}y_2(t) = D_1 g_2(x^*, x^*, \tau^*)y_1(t) + D_2 g_2(x^*, x^*, \tau^*)y_1(t - \tau^*) \\ \quad + D_3 g_2(x^*, x^*, \tau^*)y_2(t). \end{cases} \quad (12)$$

Note that the last terms in these equations are due to the explicit dependence of f_2 and g_2 on τ .

Stability of a steady state solution of Eq. (3) is analyzed using (12) combined with (4). In this case, the characteristic equation corresponding to (12) always has a zero root (a consequence of differentiating the integral condition) and hence the stability of the zero solution of (12) is not completely equivalent to the stability of the steady state of (3). However, the steady state is asymptotically stable if zero is a simple root while all other roots of the characteristic equation have negative real part.

2.2 Periodic solutions

2.2.1 Existence

Existence of periodic solutions for particular cases of sd-DDEs was proven in [23, 32, 26, 27, 2, 34]. Apart from restricting to (specific) scalar equations, these results are further restricted in the following way. Let the equation under study depend on a parameter γ . Through linearizing the equation around a steady state solution a characteristic equation is obtained. In general, an infinite number of parameter values γ_m , $m \in \mathbb{N}$, can be found, for which the characteristic equation has two pure imaginary solutions, $\pm i\omega_m$. Suppose that $\omega_m > 0$, $m = 0, 1, \dots$ are numbered in ascending order. Existence of *slowly oscillating periodic solutions* (SOP solutions) with period $T(\gamma)$, $T(\gamma_m) = 2\pi/\omega_m$, was proven only for $m = 0$ (under some additional appropriate assumptions). Recall that a periodic solution is called an SOP solution if its zeros are separated by distances greater than the maximum value of the delay function. In general, there may be periodic solutions which are not SOP solutions [27].

The theorems on existence of periodic solutions suggest that a Hopf bifurcation theorem holds for the equations under study (as pointed out, e.g., in [26]). In the following we will refer to the situation when the characteristic equation has a pair of pure imaginary roots of multiplicity 1 as a *Hopf-like* bifurcation.

Note that if all functions involved in the definition of a sd-DDE are arbitrary smooth, then a periodic solution of the equation is arbitrary smooth due to its periodicity and smoothing property of the solution operator (for the latter see, e.g., [29, 17, 33]).

2.2.2 Stability

In the case of DDEs with constant delays, the local stability of a periodic solution (with period T) is determined by the spectrum of the solution operator, $S(T, 0)$, of the linear variational equation. The operator $S(T, 0)$ equals the Fréchet derivative of the solution operator to the nonlinear (original) equation with respect to initial data (see [19], Theorem II.4.1).

The stability theory of periodic solutions of sd-DDEs has not yet been fully developed in the mathematical literature. However, continuous differentiability of solutions (and hence of the solution operator) with respect to initial data was investigated in [6, 21] for nonautonomous sd-DDEs. It was proven that the Fréchet derivative of the solution operator to the nonlinear sd-DDE with respect to initial data equals the solution operator of the linearized equation. Based on these results we linearize Eqs. (1) and (2) around a (nonconstant) solution $(x^*(t), \tau^*(t))$ as

$$\begin{aligned} \frac{d}{dt}y(t) = & D_1 f_1(s)y(t) - D_2 f_1(s) \frac{d}{dt}x^*(t - \tau(x^*(t))) \frac{\partial}{\partial x} \tau(x^*(t))y(t) \\ & + D_2 f_1(s)y(t - \tau(x^*(t))) \end{aligned} \quad (13)$$

with $s = (x^*(t), x^*(t - \tau(x^*(t))))$, respectively,

$$\begin{cases} \frac{d}{dt}y_1(t) = D_1f_2(s)y_1(t) + D_2f_2(s)y_1(t - \tau^*(t)) - D_2f_2(s)\frac{d}{dt}x^*(t - \tau^*(t))y_2(t) \\ \quad + D_3f_2(s)y_2(t) \\ \frac{d}{dt}y_2(t) = D_1g_2(s)y_1(t) + D_2g_2(s)y_1(t - \tau^*(t)) - D_2g_2(s)\frac{d}{dt}x^*(t - \tau^*(t))y_2(t) \\ \quad + D_3g_2(s)y_2(t) \end{cases} \quad (14)$$

with $s = (x^*(t), x^*(t - \tau^*(t)), \tau^*(t))$.

The proofs [6, 21] are given under a set of assumptions which concern (continuous) differentiability of the right hand side of the equation under study and the delay function. Also, a space of absolutely continuous functions is used as the state space of solutions and a quite rigorous condition on the delay function τ ,

$$\frac{d}{dt}\tau(t, x(t)) < 1 \text{ (almost everywhere),} \quad (15)$$

was required to establish the result. The latter yields the fact that $(t - \tau(t, x(t)))$ is an increasing function, or, in other words, that the amount of past that is taken into account never increases.

Eqs. (13)-(14) are linear equations with *time-dependent* (no longer state-dependent) delay. If the coefficients in the linear equation are smooth and periodic (with period T) and the delay function is smooth, then this equation belongs to the class of linear periodic equations studied in [19]. For these equations, the solution operator over the period T (over an interval mT if $r > T$ and $mT \geq r$, $m \in \mathbb{N}$, $r = \max_{t \in [0, T]} \tau(t)$) is compact. Recall that the spectrum of a compact operator consists of a point spectrum with zero as its only cluster point.

An open question remains whether the stability of the linear variational equation reflects the *local stability* of the solution $(x^*(t), \tau^*(t))$ of the corresponding nonlinear equation. In the remainder of this paper we study the *linearized stability* of periodic solutions using (13) and (14) around a periodic solution $(x^*(t), \tau^*(t))$ both in situations where assumption (15) holds and is violated.

Note that compactness of the nonlinear solution operator to a particular case of Eq. (1) was proven in [34]. In [2] the compactness of the nonlinear operator was achieved for an equation related to (2) with f_2 depending only on the solution in the past.

3 Numerical Methods

The numerical methods we use for bifurcation analysis of sd-DDEs are extensions of corresponding methods for systems of DDEs with multiple constant delays, see [24, 16, 14, 15, 11, 12]. Here we briefly present the main ideas and concentrate on changes caused by the state dependence of the delay.

3.1 Steady state solutions

A steady state solution, (x^*, τ^*) , of Eqs. (1)-(3) is determined from the following determining system

$$\begin{cases} f(x^*, \tau^*) = 0 \\ g(x^*, \tau^*) = 0, \end{cases} \quad (16)$$

where f and g are defined by (8)-(10), respectively. System (16) is a nonlinear system of algebraic equations and it can be solved by a Newton iteration starting from an initial guess for (x^*, τ^*) .

The stability of a steady state solution is determined by the roots of the characteristic equation. Let $\Delta(\lambda)$ be a characteristic matrix,

$$\Delta(\lambda) := \lambda I - A_0 - A_1 e^{-\lambda \tau^*},$$

with I the identity matrix and

$$A_0 := D_1 f_1(x^*, x^*), \quad A_1 := D_2 f_1(x^*, x^*)$$

for Eq. (1) and

$$A_0 := \begin{pmatrix} D_1 f_2(x^*, x^*, \tau^*) & D_3 f_2(x^*, x^*, \tau^*) \\ D_1 g_2(x^*, x^*, \tau^*) & D_3 g_2(x^*, x^*, \tau^*) \end{pmatrix}, \quad A_1 := \begin{pmatrix} D_2 f_2(x^*, x^*, \tau^*) & 0 \\ D_2 g_2(x^*, x^*, \tau^*) & 0 \end{pmatrix}$$

for Eq. (2) and Eq. (3) combined with (4). In general, the characteristic equation,

$$\det(\Delta(\lambda)) = 0, \quad (17)$$

has infinitely many roots. A Newton iteration can be used to find solutions of (17). However, even if a fine grid of starting values is used this gives no guarantee to find all rightmost (stability determining) roots of (17).

Approximation to the rightmost roots can be computed in the following way. Let $S(h, 0)$ be the time integration operator of the variational equation ((11) or (12)),

$$\frac{d}{dt} y(t) = A_0 y(t) + A_1 y(t - \tau^*), \quad (18)$$

i.e., $S(h, 0)y_0 = y_h$, where $y_h(s) = y(h + s)$, $s \in [-\tau^*, 0]$ and y_0, y_h are solution segments of a solution y to (18). The eigenvalues μ of $S(h, 0)$ are of the form $\mu = \exp(\lambda h)$, with λ a solution of (17), plus possibly zero. Selected eigenvalues of $S(h, 0)$ can be approximated by discretizing $S(h, 0)$ to a matrix and by using established numerical algorithms to compute selected eigenvalues of (possibly very large) matrices. Once an eigenvalue μ of $S(h, 0)$ is found, the corresponding root of the characteristic equation can be extracted using $\Re(\lambda) = \log(|\mu|)/h$ and $\Im(\lambda) = (\arcsin(\Im(\mu)/|\mu|)/h) \bmod \pi/h$. The full imaginary part can further be extracted from the corresponding eigenvector of $S(h, 0)$.

To discretize $S(h, 0)$, we use a linear multi-step formula. More details on this method and the effect of the discretization can be found in [22, 18, 12]. The approximated rightmost roots λ can further be corrected using a Newton iteration on the system

$$\begin{cases} \Delta(\lambda)v = 0 \\ c^T v - 1 = 0, \end{cases} \quad (19)$$

where a starting value for v is the eigenvector of $\Delta(\lambda)$ corresponding to its smallest eigenvalue (in modulus) and the last equation is a suitable normalization of v .

Note that in the case of the threshold-delay equation (3), we use determining system (16) (and hence the threshold condition in (3)) to compute a steady state solution, but we use the linearization of (2) combined with (4) for the stability analysis.

Dependence of the steady state (x^*, τ^*) on a physical parameter can be studied by computing a branch of steady state solutions as a function of the parameter using a continuation procedure (see, e.g., [10] and for DDEs [11]). The stability of the steady state can change during continuation whenever eigenvalues of $\Delta(\lambda)$ cross the imaginary axis. Hence monitoring the rightmost eigenvalues along the branch allows detection of bifurcations.

Hopf-like bifurcations can be computed using the following determining system [24],

$$\begin{cases} f(x^*, \tau^*, \gamma) = 0 \\ g(x^*, \tau^*, \gamma) = 0 \\ \Delta(x^*, \tau^*, \gamma, i\omega)v = 0 \\ c^T v - 1 = 0, \end{cases} \quad (20)$$

where $\omega \in \mathbb{R}$, $v \in \mathbb{C}^n$ and γ is a physical parameter which is allowed to change during Newton iteration. A branch of Hopf-like bifurcation points can then be continued in a two-parameter space.

3.2 Periodic solutions

Let $x_t(\theta) = x(t + \theta)$, $\theta \in [-r, 0]$, where r is the maximum value of the delay. A solution of a DDE is uniquely determined by a function segment on the delay interval while a solution of an ordinary differential equation (ODE) is uniquely determined by its value at one point. Hence the periodicity conditions for DDEs and ODEs are $x_0 = x_T$, respectively, $x(0) = x(T)$ with T the period of the solution $x(t)$.

3.2.1 Periodic boundary value problems

Periodic solutions of Eqs. (1)-(3) can be found as solutions of the following *two-point boundary value problems* (BVPs),

$$\begin{cases} \frac{d}{dt}x(t) = f_1(x(t), x(t - \tau(x(t))))), & t \in [-r, T] \\ x_0 = x_T \\ s(x, T) = 0, \end{cases} \quad (21)$$

respectively,

$$\begin{cases} \frac{d}{dt}x(t) = f_2(x(t), x(t - \tau(t)), \tau(t)) \\ \frac{d}{dt}\tau(t) = g_2(x(t), x(t - \tau(t)), \tau(t)), & t \in [-r, T] \\ x_0 = x_T \\ \tau(0) = \tau(T) \\ s(x, \tau, T) = 0 \end{cases} \quad (22)$$

and

$$\begin{cases} \frac{d}{dt}x(t) = f_3(x(t), x(t - \tau(t)), \tau(t)) \\ \frac{d}{dt}\tau(t) = 1 - \frac{g_3(x(t))}{g_3(x(t - \tau(t)))}, & t \in [-r, T] \\ x_0 = x_T \\ \int_{-\tau(0)}^0 g_3(x(s))ds - 1 = 0 \\ s(x, \tau, T) = 0. \end{cases} \quad (23)$$

Here T is the (unknown) period, $r \geq \max_{t \in [0, T]} \tau(t)$ is given and s is a suitable phase condition to remove the indeterminacy due to the fact that a phase shift of any periodic solution is also a periodic solution.

In (21), the delay function, $\tau(x(t)) = g_1(x(t))$, is computed explicitly. In (22), the delay τ is determined by an ordinary differential equation with respect to τ . Hence we also need a periodicity condition for τ , $\tau(0) = \tau(T)$. To compute a periodic solution of Eq. (3) in a standard way (through a periodic BVP for DDEs), we differentiate the threshold condition in (3). The periodicity condition for τ is replaced by the integral condition for $t = 0$. In this way, BVP (23) uniquely determines a periodic solution to (3).

3.2.2 Collocation approximation

To compute solutions to (21)-(23), we use a collocation method based on piecewise polynomials. In [14], we investigated collocation methods for the computation of periodic solutions of systems of DDEs with constant delays. The approach has been shown to be quite efficient and we use it for the case of state-dependent delay. We explain the main idea for BVP (23).

The solution profile x and the delay function τ are approximated by piecewise polynomials $u(t)$, respectively $v(t)$, on the interval $[0, 1]$. The functions $u(t)$ and $v(t)$ are represented on each interval of a mesh $0 = t_0 < t_1 < \dots < t_L = 1$ as polynomials of degree m ,

$$u(t) = \sum_{j=0}^m u(t_{i+\frac{j}{m}}) P_{i,j}(t), \quad t \in [t_i, t_{i+1}], \quad i = 0, \dots, L-1, \quad (24)$$

where

$$P_{i,j}(t) = \prod_{k=0, k \neq j}^m \frac{t - t_{i+\frac{k}{m}}}{t_{i+\frac{j}{m}} - t_{i+\frac{k}{m}}}, \quad j = 0, \dots, m-1 \quad (25)$$

are Lagrange polynomials and $t_{i+j/m} = t_i + \frac{j}{m}h_i$, $h_i := t_{i+1} - t_i$. Similar formulas hold for $v(t)$.

Let $X := \{c_{i,l} := t_i + c_l h_i, i = 0, 1, \dots, L-1, l = 1, \dots, m\}$ be a given set of collocation points based on the collocation parameters $0 \leq c_1 < c_2 < \dots < c_m \leq 1$. The collocation solutions $u(t)$ and $v(t)$ are determined in terms of the unknowns $u_{i+j/m} := u(t_{i+j/m})$, $v_{i+j/m} := v(t_{i+j/m})$, $i = 0, \dots, L-1$, $j = 0, \dots, m-1$ and $u_L := u(t_L)$, $v_L := v(t_L)$ by collocation equations which, for u , read

$$\frac{d}{dt}u(c_{i,l}) = T f_3(u(c_{i,l}), u((c_{i,l} - \frac{v(c_{i,l})}{T}) \bmod 1), v(c_{i,l})). \quad (26)$$

Similar formulas hold for v .

In (26), time was scaled by the factor T^{-1} (to obtain a periodic solution on the interval $[0, 1]$) and we used the periodicity condition to eliminate $u(t)$ for $t < 0$. Note that we allow, using the modulo operation, the period T to be less than the delay. Using $c = c_{i,l}$ and $\tilde{c} = (c - v(c)/T) \bmod 1$, $t_k \leq \tilde{c} < t_{k+1}$, the collocation equations have the following structure

$$\begin{cases} \sum_{j=0}^m u_{i+\frac{j}{m}} P'_{i,j}(c) = T f_3(\sum_{j=0}^m u_{i+\frac{j}{m}} P_{i,j}(c), \sum_{j=0}^m u_{k+\frac{j}{m}} P_{k,j}(\tilde{c}), \\ \quad \sum_{j=0}^m v_{i+\frac{j}{m}} P_{i,j}(c)), \\ \sum_{j=0}^m v_{i+\frac{j}{m}} P'_{i,j}(c) = T(1 - g_3(\sum_{j=0}^m u_{i+\frac{j}{m}} P_{i,j}(c))/g_3(\sum_{j=0}^m u_{k+\frac{j}{m}} P_{k,j}(\tilde{c}))), \end{cases} \quad (27)$$

where $P'_{i,j}$ denotes the derivative of $P_{i,j}$. We did not eliminate u_0 and v_0 because these values are used in $[0, t_1]$. So we still need to require $u_0 = u_L$ and $v_0 = v_L$. Because of the special form of (23) periodicity of v follows from periodicity of u and we replace the latter condition by the integral condition,

$$\int_{1-\tau(1)/T}^1 g_3(x(s)) ds - 1 = 0, \quad (28)$$

which is equivalent to the one in (23) and can be discretized using a quadrature formula based on the unknowns $u_{i+j/m}$, u_L and v_L , where $k \leq i \leq L-1$, $j = 0, 1, \dots, m-1$ and k is such that $t_k \leq 1 - v_L/T < t_{k+1}$.

The system of collocation equations (27) together with equations $u_0 = u_L$, $s(u, v, T) = 0$ and an approximation of the integral condition (28) are solved iteratively by a Newton iteration. Note that the period T is also computed within the Newton iteration. The latter corresponds with the fact that we obtained a $(n(Lm+1)+1)$ -dimensional system with $n(Lm+1)$ collocation unknowns and the unknown T . We do not present here the linearization of collocation equation (27) (which is in agreement with the linearization (14)) because it is a long and tedious formula.

For BVPs (21) and (22), the collocation approximation is similar. For (21), the only difference is in determining the point in the past, $\tilde{c} = (c - \tau(c)/T) \bmod 1$, where $\tau(c) = g_1(u(c))$. For (22), we need to require $v_0 = v_L$.

A branch of periodic solutions can be traced as a function of a system parameter using a continuation procedure. The branch can be started from a Hopf-like point

detected through the stability analysis of steady state solutions or from an initial guess (e.g., resulting from time integration).

3.2.3 Linear stability analysis

We study the linearized stability of a periodic solution $(x^*(t), \tau^*(t))$ as determined by the spectrum of the (linear) solution operator $S(T, 0)$ which integrates the variational equation ((13) or (14)) around $(x^*(t), \tau^*(t))$ from time $t = 0$ over the period T . Any nonzero eigenvalue μ of the operator $S(T, 0)$ is called a characteristic (Floquet) multiplier of the variational equation. Furthermore, $\mu = 1$ is always an eigenvalue of $S(T, 0)$ and it is referred to as the trivial Floquet multiplier. A discrete approximation of $S(T, 0)$, a matrix M , is obtained using the collocation equations (e.g., (27) for BVP (23)) without the modulo operation for the delayed argument. M is constructed as a map of the variables representing the segment $[-r, 0]$ to the variables representing the segment $[T - r, T]$, where $r = \max_{t \in [0, T]} \tau^*(t)$. The eigenvalues of M form approximations to the Floquet multipliers.

4 Examples

We apply the numerical methods described in Sec. 3 to analyze solutions of two differential equations with state-dependent delay.

4.1 Example 1

The following equation is of type (1),

$$\begin{cases} \frac{d}{dt}x(t) = -kx(t - \tau(x(t))) \\ \tau(x) = \alpha e^{-x^2} + 1 - \alpha. \end{cases} \quad (29)$$

It was studied in [23, 27] for $k > 0$, $\alpha \in [0, 1]$. The equation has a unique steady state solution, $(x^*, \tau^*) = (0, 1)$. Linearization of (29) around the steady state (see Sec. 2.1) yields a characteristic equation,

$$\lambda + ke^{-\lambda} = 0. \quad (30)$$

Equation (30) has pure imaginary roots $\lambda_m = \pm i\omega_m$, $\omega_m = \pi/2 + 2\pi m$ for $k_m = \omega_m$, $m \in \mathbb{N}$. The steady state is unstable for $k > \pi/2$. The existence of SOP solutions to (29) was proven in [23, 27] for $k > \pi/2$ and $k < 3$. However, the latter condition is too strict and numerical simulations suggest existence of SOP solutions to (29) for a much larger range of k (see [23, 27]). Equation (29) is a particular case of the type of equations for which compactness of the solution operator was proven in [34].

4.2 Example 2

The following threshold-type equation,

$$\begin{cases} \frac{d}{dt}x(t) = -\nu x(t) + \gamma e^{-\beta\tau(t)} \frac{P(x(t))}{P(x(t-\tau(t)))} x(t - \tau(t)) \\ \int_{t-\tau(t)}^t P(x(s)) ds = 1, \end{cases} \quad (31)$$

was studied in [31] for a quite general class of functions $P(x)$ which includes

$$P(x) = c_1 e^{-c_2 x},$$

used in our numerical analysis in Sec. 5.2. Here $\nu, \gamma, \beta, c_1, c_2$ are positive parameters. In [31], Eq. (31) was obtained by a reduction of a structured population model (a system of a partial and an ordinary differential equation) taken from [28]. The model describes the time evolution of a mature population size $x(t)$. The threshold condition implies that the delay τ (the amount of time spent in the immature class by the cohort that matures at time t) depends on the past history of the mature population size through $P(x)$.

In [31], the author transforms the threshold-delay equation to a scalar DDE with one constant delay and distributed delay by a solution-dependent change of the independent variable. The stability of both the zero and the nonzero steady state solution of the obtained equation is examined using the well-known linear stability analysis for DDEs with state-independent delay. It is found that the zero solution, $x^* = 0$ with $\tau^* = 1/c_1$, is stable if $\nu > \gamma \exp(-\beta/c_1)$. At $\nu = \gamma \exp(-\beta/c_1)$ a transcritical bifurcation occurs, i.e. the zero and the nonzero solutions intersect and interchange stability. Furthermore, for the zero state there always exists a simple real root λ_0 such that $\Re(\lambda) < \lambda_0$ for all other roots λ . The latter implies that periodic solutions bifurcating from the zero state are always unstable. Stability region of the nonzero solution in a two-parameter space was obtained using conditions for Hopf bifurcations.

Proofs concerning the validity of the transformation are not published. Note that the characteristic equation which we obtain using the linearization (12) agrees with the one established through this approach.

5 Numerical Results

Throughout this section a (periodic) collocation solution is denoted by $(x(t), \tau(t))$. In the collocation method, we used Gauss-Legendre collocation points, $m = 3$ and adaptive meshes (unless explicitly mentioned otherwise) with different number of subintervals, $20 \leq L \leq 600$. For adaptive mesh selection we used the strategy outlined in [4, 14].

By stability (instability) of computed periodic solutions we mean stability (instability) of the zero solution of the corresponding linear variational equation around the periodic solution. If no unstable modes were found, the stability of the computed periodic solution was checked using time integration with the package Archi [30]. All

time integration tests performed indicate the correspondence of the linear stability analysis with the local stability under the corresponding nonlinear equation.

5.1 Example 1

In this section, we present results on the computation of a branch of stable (Fig. 1) and a branch of unstable (Fig. 2) periodic solutions of (29) bifurcating from the steady state $(x^*, \tau^*) = (0, 1)$ for $\alpha = 0.5$ and $k = \pi/2$, respectively, $k = \pi/2 + 2\pi$. The condition $\max_{t \in [0, T]} d\tau(t)/dt < 1$ (see Sec. 2.2.2) holds at every point on the unstable branch but is violated on the stable branch when $k > \tilde{k}$, $\tilde{k} \approx 1.620$. Nothing special was observed when the condition failed to be fulfilled.

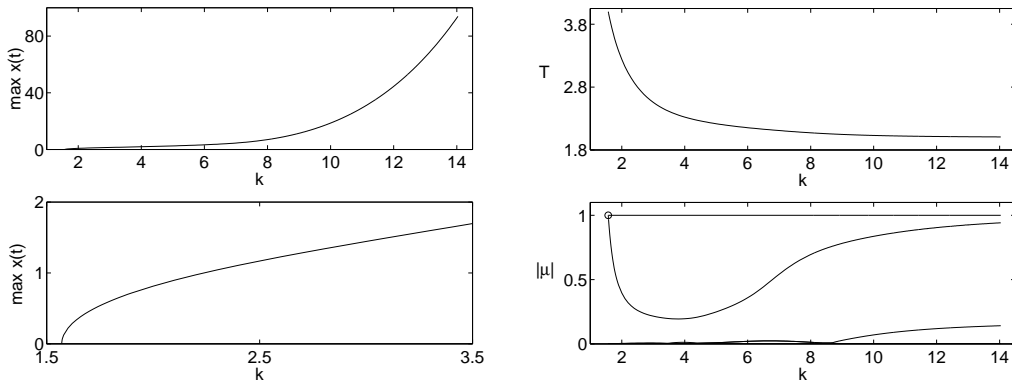


Figure 1: Evolution of $\max_{t \in [0, T]} x(t)$ (left), the period T (right, top) and moduli of the computed dominant Floquet multipliers μ (right, bottom) along a branch of stable periodic solutions of Eq. (29). \circ - Hopf-like bifurcation. Left: the lower figure is an enlargement of the upper figure.

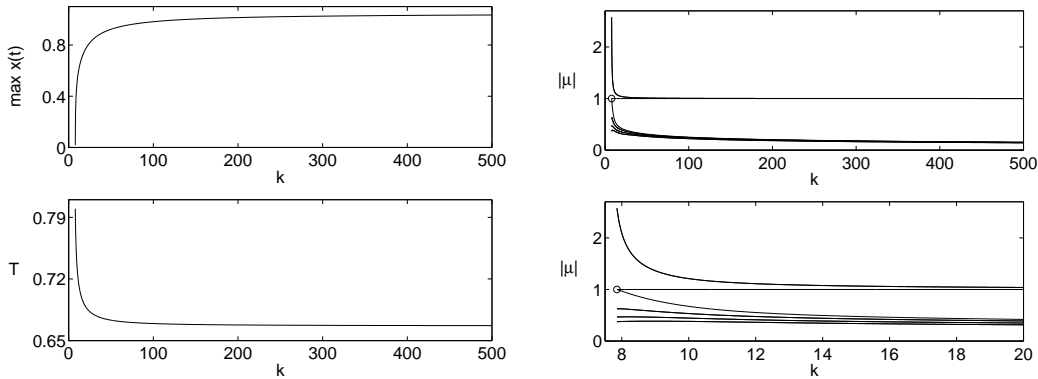


Figure 2: Evolution of $\max_{t \in [0, T]} x(t)$ (left, top), the period T (left, bottom) and moduli of the computed dominant Floquet multipliers μ (right) along a branch of unstable periodic solutions of Eq. (29). \circ - Hopf-like bifurcation. Right: the lower figure is an enlargement of the upper figure.

The stable periodic solutions are SOP solutions because $\max_{t \in [0, T]} \tau(x(t)) = 1$

and $T > 2$ holds along the branch while unstable periodic solutions are not SOP solutions ($T < 2$ along the branch). The results on stable periodic solutions confirm the hypothesis (made in [23, 27]) about the existence of SOP solutions for $k > 3$. Note that along the stable and the unstable branch T tends to 2, respectively, $2/3$ as k increases. These limit values cannot be reached due to restrictions on the period, $T \neq 2/(2j - 1)$, $j = 1, 2, 3, \dots$. Indeed, all computed periodic solutions are symmetric ($x(t + T/2) = -x(t)$) and if $x(t_1) = 0$ and $dx(t_1)/dt \neq 0$ ($t_1 \in [0, T]$), then $x(t_1 + jT - \tau(x(t_1))) = x(t_1 + jT - 1) \neq 0$. Hence the distance between two successive zeros, $T/2$, of $x(t)$ cannot equal $jT - 1$.

The stability of the periodic solutions does not change along the computed branches although the modulus of the most dominant (pair of complex) multipliers for the unstable branch approaches 1 near the end of the computed branch, $|\mu| \approx 1.0014$ at $k = 500$. For this multiplier, it seems likely that $|\mu| \rightarrow 1$ as $k \rightarrow \infty$ without ever reaching it.

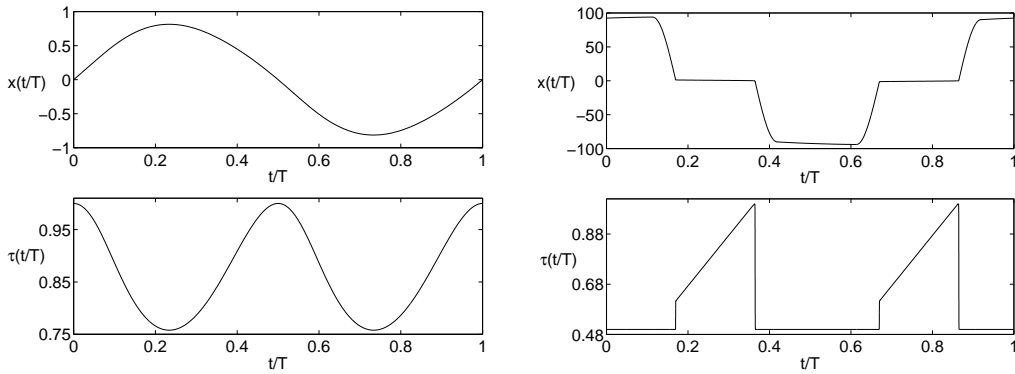


Figure 3: The profile of a stable periodic solution, $x(t/T)$, and the delay function, $\tau(t/T)$, at two points on the branch shown in Fig. 1, $k = 2$ (left) and $k = 14$ (right).

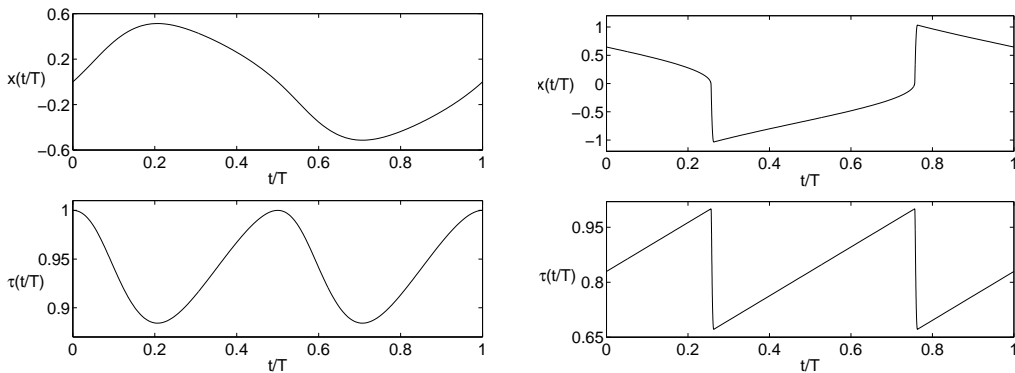


Figure 4: The profile of an unstable periodic solution, $x(t/T)$, and the delay function, $\tau(t/T)$, at two points on the branch shown in Fig. 2, $k = 10$ (left) and $k = 500$ (right).

During continuation of both branches, steep gradients occur in the derivative of

the periodic solutions as k increases (see Figs. 3-4). To prevent loss of accuracy, we increased the number of subintervals of the mesh, L . In particular, we used meshes with $L = 600$ and $L = 200$ at the end of the stable and unstable branches, respectively. For such large mesh sizes the computational costs increase significantly. Solution profiles and delay functions in Figs. 3-4 (right) look non-smooth. However, enlargements (Fig. 5 (left)) of some “difficult” places show that solutions are smooth and that the adaptive mesh efficiently catches the difficult parts. Note that the accuracy of the trivial multiplier can be used as a first check on the accuracy of computations. On both branches, we chose the value of L such that the trivial multiplier had at least 4-5 digits of accuracy.

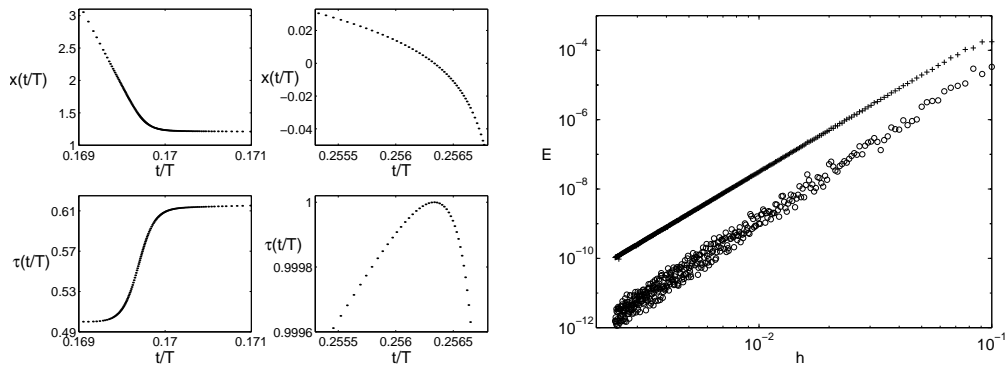


Figure 5: Left: enlargements of some parts of solutions shown in Figs. 3-4 (right). Right: evolution of E_C (+) and E_I (o) for a periodic solution on the stable branch, $k = 2$, and using equidistant meshes with $m = 3$.

In [13] convergence results were proven for collocation methods of the kind (26) for solving periodic BVPs of DDEs with constant delays. In particular, the continuous error,

$$E_C = \max_{t \in [0,1]} \|x^*(Tt) - x(t)\|,$$

is $\mathcal{O}(h^{m+1})$ when using Gauss-Legendre collocation points. Here x^* denotes the exact periodic solution, x the collocation solution, and $\|\cdot\|$ is the Euclidean norm. We numerically observed the same result for Eq. (29). Figure 5 (right) shows the evolution of the continuous error E_C and the discrete error E_I ,

$$E_I = \max_{i=0,\dots,L} \|x^*(Tt_i) - x(t_i)\|,$$

as $h \rightarrow 0$, where $h = 1/(L - 1)$. A reference solution for x^* was computed using $L = 1300$. We compared x^* to x (for $L = 10, \dots, 250$) at a very fine mesh in order to compute E_C , and at (only) the mesh points in order to compute E_I . The slope of E_C was approximated by means of a least squares fit on (all) the results for $L = 100, \dots, 250$. The result, $s \approx 3.996$, clearly indicates $\mathcal{O}(h^{m+1})$ convergence behaviour.

5.2 Example 2

This section contains results on the computation, stability analysis and continuation of steady state and periodic solutions of Eq. (31). Note that parameter c_2 does not affect the stability of solutions and we used $c_2 = 1$ throughout all computations.

5.2.1 Steady state solutions

We fixed the parameters of Eq. (31) and computed the nonzero steady state, (x^*, τ^*) , as a solution of Eq. (10), i.e.,

$$\begin{cases} -\nu + \gamma e^{-\beta\tau^*} = 0 \\ \tau^* c_1 e^{-c_2 x^*} - 1 = 0. \end{cases} \quad (32)$$

Figure 6 shows the rightmost roots of the characteristic equation corresponding to the variational equation (12) at the computed steady state. The steady state is unstable due to a complex pair of eigenvalues, $\lambda \approx 7.7e-03 \pm 0.48i$. A zero eigenvalue is a consequence of differentiating the threshold condition. We continued a branch of steady state solutions starting from (x^*, τ^*) by varying the parameter ν , see Fig. 7. During continuation we detected two Hopf-like bifurcations and the transcritical bifurcation. At the latter, the solution (x^*, τ^*) crosses the point $(0, 1/c_1)$, see Fig. 7 (left).

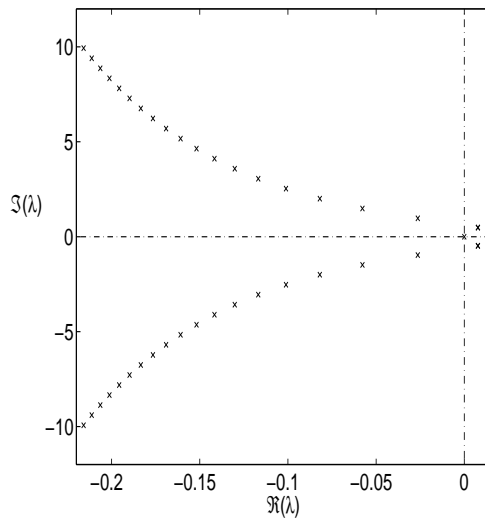


Figure 6: Rightmost roots of the characteristic equation at the steady state $(x^*, \tau^*) \approx (1.33, 11.87)$ of Eq. (31). $c_1 = 1/\pi$, $\nu \approx 0.33$, $\gamma \approx 47.67$, $\beta \approx 0.42$.

Starting from the first Hopf-like point (Fig. 7), we continued a branch of Hopf-like bifurcation points in the (β, ν) -parameter space, see Fig. 8 (left, top). Then we used a point on the computed branch to continue a branch of Hopf-like points in the (γ, ν) -parameter space, see Fig. 8 (left, bottom) and so on. The indicated branches of transcritical bifurcations were obtained analytically (see Sec. 4.2).

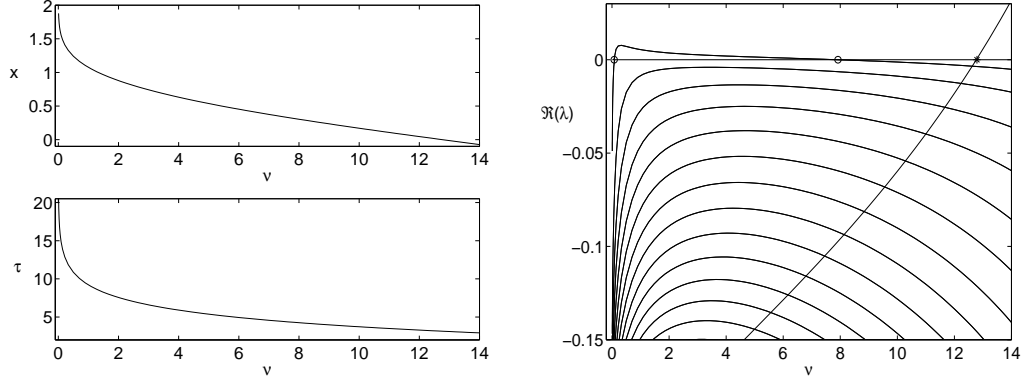


Figure 7: The solution (x, τ) (left) and real part of the rightmost roots of the characteristic equation (right) along a branch of steady state solutions of Eq. (31) versus parameter ν . $c_1 = 1/\pi$, $\gamma \approx 47.67$, $\beta \approx 0.42$. o - Hopf-like bifurcation ($\nu \approx 0.079$, $\nu \approx 7.92$), * - transcritical bifurcation ($\nu \approx 12.79$).

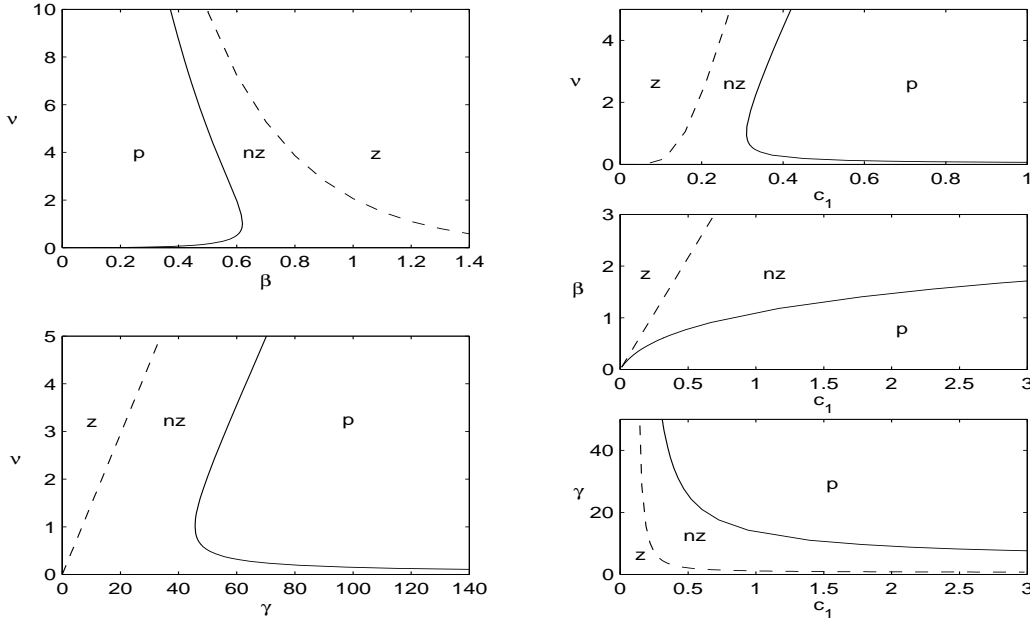


Figure 8: Regions of stability of the zero (z), nonzero (nz) steady state and periodic solutions (p) of Eq. (31) in several two-parameter spaces. $c_1 = 1/\pi$, $\gamma \approx 47.67$ (left, top), $c_1 = 1/\pi$, $\beta \approx 0.61$ (left, bottom), $\gamma \approx 47.67$, $\beta \approx 0.61$ (right, top), $\nu \approx 0.63$, $\gamma \approx 47.67$ (right, middle), $\nu \approx 0.63$, $\beta \approx 0.61$ (right, bottom). Solid lines denote Hopf-like bifurcation branches and dashed lines denote transcritical bifurcation branches.

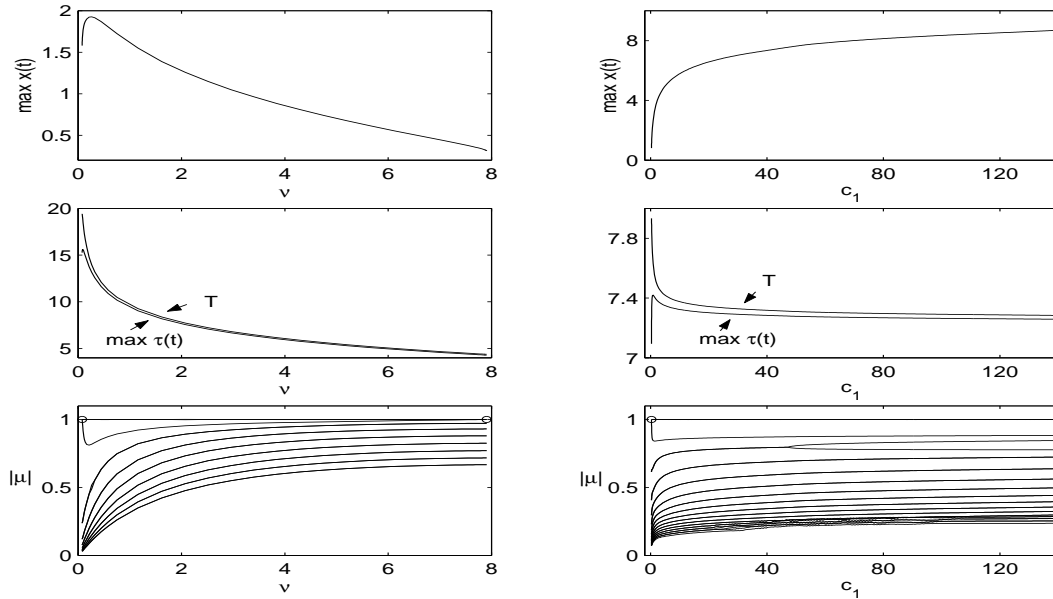


Figure 9: Evolution of $\max_{t \in [0, T]} x(t)$, the period T , $\max_{t \in [0, T]} \tau(t)$ and moduli of the computed dominant Floquet multipliers along two branches of periodic solutions of Eq. (31). \circ - Hopf-like bifurcation. $\gamma \approx 47.67$. Left: $c_1 = 1/\pi$, $\beta \approx 0.42$. Right: $\nu \approx 0.63$, $\beta \approx 0.61$.

5.2.2 Periodic solutions

We computed a number of branches of periodic solutions versus parameters of (31). No bifurcations of periodic solutions were found. The condition $d\tau(t)/dt < 1$ holds for all periodic solutions of this equation due to the type of threshold condition. Two multipliers are constant at 1 along the computed branches. One of these is the trivial Floquet multiplier and the second is a consequence of differentiating the integral equation. During continuation multipliers usually tend to 1 rather slowly and steep gradients often occur in the derivative of solutions. The latter leads to loss of accuracy of the computed Floquet multipliers, see further. Test results similar to those shown in Fig. 5 again indicate that the collocation method used produces continuous errors of order $\mathcal{O}(h^{m+1})$.

Figure 9 (left) depicts a branch of periodic solutions as a function of ν which emanates from the first Hopf-like point in Fig. 7. In agreement with Fig. 7, the branch ends at a second Hopf-like point. During continuation, the maximal value of the delay becomes close to (but remains slightly less than) the period T ($\tau(t) = T$ is not possible due to the threshold condition). The shape of the solution profile (e.g., Fig. 10 (left)) does not change significantly along the branch. In this case, a small number of mesh subintervals, $L=40$, was sufficient to obtain good accuracy of the computed solutions and multipliers.

To study the influence of the threshold condition on the behaviour of solutions, we computed a branch of periodic solutions as a function of parameter c_1 , see Fig. 9 (right). The branch starts from a Hopf-like point on the branch shown in Fig. 8

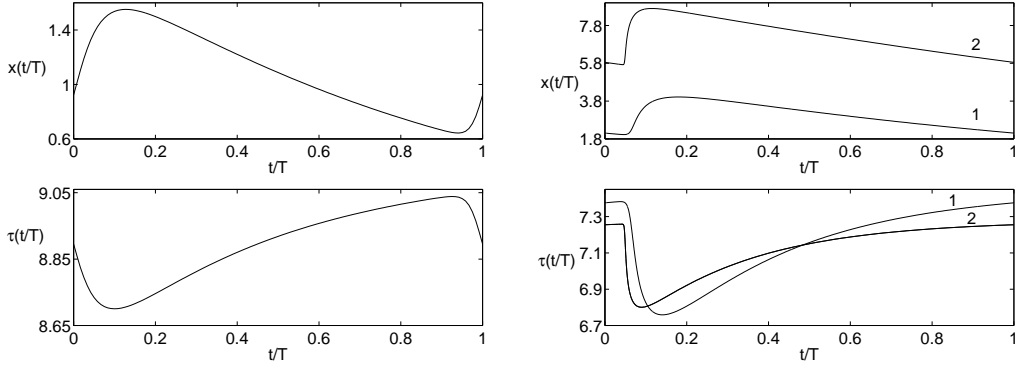


Figure 10: Profiles of periodic solutions. Left: a point on the branch shown in Fig. 9 ($\nu \approx 1.16$). Right: two points on the branch shown in Fig. 9 ($c_1 \approx 2.36$ (1), $c_1 = 140$ (2)).

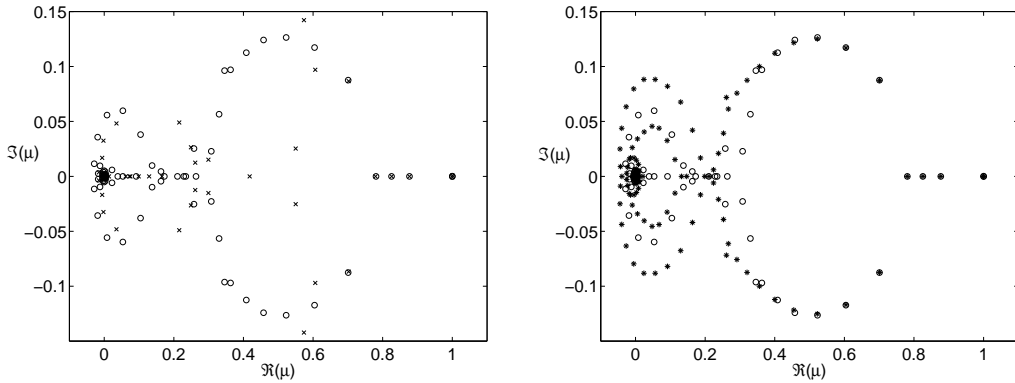


Figure 11: The computed Floquet multipliers for a point on the branch shown in Fig. 9 (right, $c_1 \approx 70.23$) with $L = 40$ (x), $L = 100$ (o) (left) and with $L = 100$ (o), $L = 200$ (*) (right).

(right, top, $c_1 = 1/\pi$) and it remains stable during continuation. Away from the Hopf-like point, the solution profiles rapidly develop steep gradients in the derivative and the steepness increases along the branch. Examples of two solution profiles are given in Fig. 10 (right). An adaptive mesh with $L = 200$ subintervals was used from the beginning of the branch. Figure 11 shows the Floquet multipliers for a point on the branch computed for different values of L . Convergence behaviour is apparent and $L = 200$ gives good accuracy even for small multipliers.

The evolution of the solution profile during continuation can be explained in the following way. An increase of c_1 is equivalent to a decrease of the threshold itself. To satisfy the latter, the function under integral, ($\exp(-c_2 x(t))$), as well as the delay $\tau(t)$ have to decrease too, which leads to an increase of the solution $x(t)$ and a decrease of $\tau(t)$ over the period T . Figure 10 (right) reflects these changes. The amount of growth and decrease is determined by the right hand side of Eq. (31).

Figure 12 illustrates the evolution of periodic solutions as the parameter β decreases. The difference between period T and $\max \tau(t)$ is not visible, $T - \max \tau(t) \approx$

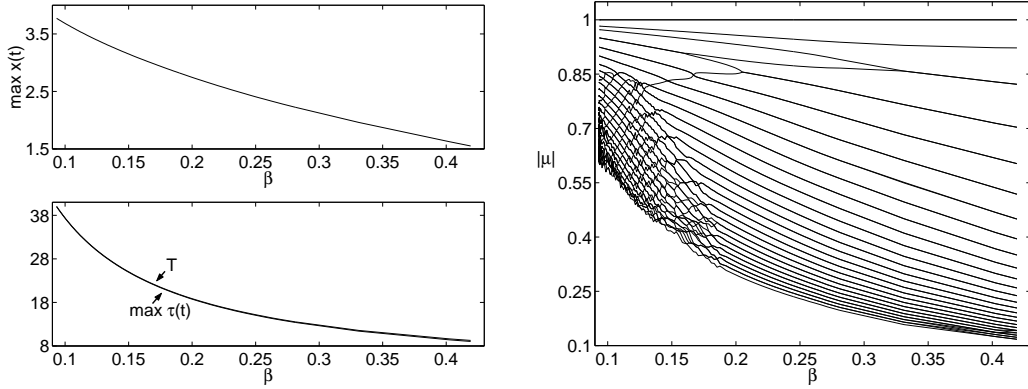


Figure 12: Evolution of $\max_{t \in [0, T]} x(t)$ (left, top), the period T , $\max_{t \in [0, T]} \tau(t)$ (left, bottom) and moduli of the computed dominant Floquet multipliers μ (right) along a branch of periodic solutions of Eq. (31). $c_1 = 1/\pi$, $\nu \approx 1.16$, $\gamma \approx 47.67$.

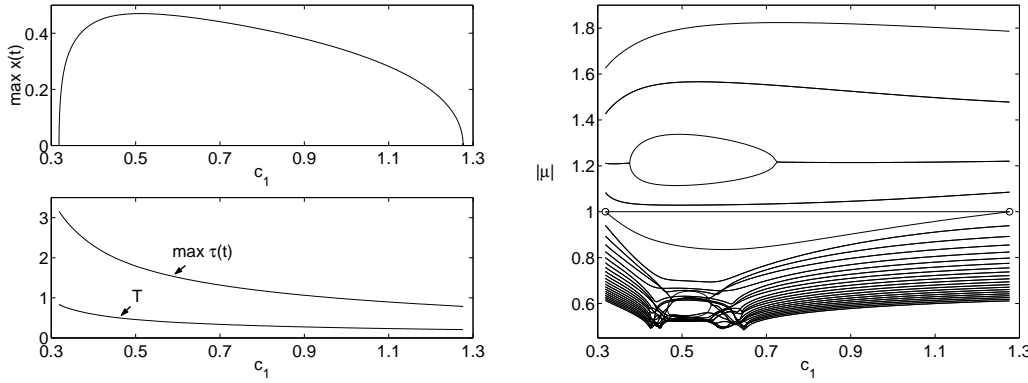


Figure 13: Evolution of $\max_{t \in [0, T]} x(t)$ (left, top), the period T , $\max_{t \in [0, T]} \tau(t)$ (left, bottom) and moduli of the computed dominant Floquet multipliers μ (right) along a branch of periodic solutions of Eq. (31). \circ - Hopf-like bifurcation ($c_1 = 1/\pi$, $c_1 \approx 1.28$). $\nu \approx 0.63$, $\gamma \approx 47.67$, $\beta \approx 0.59$.

0.0650 at the last computed point ($\beta \approx 0.0933$) on the branch. To prevent loss of accuracy of the computed dominant multipliers, we used $L = 400$ when $\beta < 0.28$. In the figure it is clearly visible that less dominant multipliers are inaccurate for small values of β .

Periodic solutions bifurcating from the zero state are always unstable (cf. Sec. 4.2). Figure 13 shows a branch of periodic solutions bifurcating from and ending at the zero steady state. Note that along the branch the maximal value of the delay is larger than the period value.

6 Conclusions

We extended existing numerical methods for bifurcation analysis of delay differential equations with constant delay [24, 16, 14, 15, 11, 12] towards equations with state-dependent delay. In this paper, we concentrated on three classes of equations: (i) the delay τ is a given (explicit) function of the solution, (ii) τ is determined by a differential equation and (iii) τ is determined implicitly by a solution segment through a threshold condition.

The theory of differential equations with state-dependent delay has been under development and is not complete yet. We collected the relevant theoretical results and pointed out open theoretical problems in the context of bifurcation analysis. In particular, stability of steady state solutions of such equations is well understood but a number of important open theoretical questions remain concerning the existence and stability of periodic solutions.

By investigating two examples, we showed computational results on steady state solutions, their stability, Hopf bifurcations and corresponding branches of periodic solutions in situations treated by the existing theory. Furthermore, we showed computed branches of periodic solutions and their stability in situations where some of assumptions of the proven results are violated. We compared computational results with analytical ones whenever possible.

The results presented show that numerical bifurcation analysis of differential equations with state-dependent delays can be successfully achieved.

Acknowledgements

This research presents results of the research project OT/98/16, funded by the Research Council K.U.Leuven, of the research project G.0270.00 funded by the Fund for Scientific Research - Flanders (Belgium) and of the research project IUAP P4/02 funded by the programme on Interuniversity Poles of Attraction, initiated by the Belgian State, Prime Minister's Office for Science, Technology and Culture. The scientific responsibility is assumed by its authors. K. Engelborghs is a research assistant of the Fund for Scientific Research - Flanders (Belgium).

References

- [1] W. G. Aiello, H. I. Freedman, and J. Wu. Analysis of a model representing stage-structured population growth with state-dependent time delay. *SIAM J. Appl. Math.*, 52(3):855–869, 1992.
- [2] O. Arino, K. P. Hadeler, and M. L. Hbid. Existence of periodic solutions for delay differential equations with state dependent delay. *J. Diff. Eqns.*, 144:263–301, 1998.

- [3] O. Arino, M. L. Hbid, and R. B. de la Parra. A mathematical model of growth of population of fish in the larval stage: density-dependence effects. *Math. Biosci.*, 150:1–20, 1998.
- [4] U. M. Ascher, R. M. M. Mattheij, and R. D. Russell. *Numerical Solution of Boundary Value Problems for Ordinary Differential Equations*. Prentice Hall, 1988.
- [5] C. T. H. Baker, G. A. Bocharov, and F. A. Rihan. A report on the use of delay differential equations in numerical modeling in the biosciences. Numerical Analysis Report 343, Manchester Centre for Computational Mathematics, University of Manchester, July 1999.
- [6] M. Brokate and F. Colonius. Linearizing equations with state-dependent delays. *Appl. Math. Optim.*, 21:45–52, 1990.
- [7] Y. Cao, J. Fan, and T. C. Gard. The effects of state-dependent time delay on a stage-structured population growth model. *Nonlinear Anal.*, 19(2):95–105, 1992.
- [8] K. L. Cooke and W. Huang. On the problem of linearization for state-dependent delay differential equations. *Proc. AMS*, 124(5):1417–1426, 1996.
- [9] S. P. Corwin, D. Sarafyan, and S. Thompson. DKL6G: A code based on continuously imbedded sixth order Runge-Kutta methods for the solution of state dependent functional differential equations. *Appl. Numer. Math.*, 24(2–3):319–330, 1997.
- [10] E. J. Doedel, H. B. Keller, and J. P. Kernevez. Numerical analysis and control of bifurcation problems (I) bifurcation in finite dimensions. *Internat. J. Bifur. Chaos*, 1(3):493–520, 1991.
- [11] K. Engelborghs. *DDE-BIFTOOL: a Matlab package for bifurcation analysis of delay differential equations*. Department of Computer Science, Katholieke Universiteit Leuven, Belgium, 2000. In preparation.
- [12] K. Engelborghs. *Numerical bifurcation analysis of delay differential equations*. Phd thesis, Department of Computer Science, Katholieke Universiteit Leuven, Belgium, 2000. In preparation.
- [13] K. Engelborghs and E. J. Doedel. Stability of piecewise polynomial collocation methods for computing periodic solutions of delay differential equations. In preparation, 2000.
- [14] K. Engelborghs, T. Luzyanina, K. in’t Hout, and D. Roose. Collocation methods for the computation of periodic solutions of delay differential equations. TW report 295, Department of Computer Science, Katholieke Universiteit Leuven, Belgium, November 1999. Submitted to *SIAM J. Sci. Comput.*

- [15] K. Engelborghs, T. Luzyanina, and D. Roose. Numerical bifurcation analysis of delay differential equations using DDE-BIFTOOL. 2000. Submitted to IMA J. Numer. Anal.
- [16] K. Engelborghs and D. Roose. Numerical computation of stability and detection of Hopf bifurcations of steady state solutions of delay differential equations. *Adv. Comput. Math.*, 10:271–289, 1999.
- [17] A. Feldstein and K. W. Neves. High order methods for state-dependent delay differential equations with nonsmooth solutions. *SIAM J. Numer. Anal.*, 21(5):844–863, 1984.
- [18] N. J. Ford. Numerical approximation of the characteristic values for a delay differential equation. Numerical analysis report 350, Manchester Centre for Computational Mathematics, Department of Mathematics, September 1999.
- [19] J. K. Hale. *Theory of Functional Differential Equations*, volume 3 of *Applied Mathematical Sciences*. Springer-Verlag, 1977.
- [20] F. Hartung and J. Turi. Stability in a class of functional differential equations with state-dependent delay. In C. Corduneanu, editor, *Qualitative problems for differential equations and control theory*, pages 15–31. World Scientific, 1995.
- [21] F. Hartung and J. Turi. On differentiability of solutions with respect to parameters in state-dependent delay equations. *J. Diff. Eqns.*, 135:192–237, 1997.
- [22] T. Hong-Jiong and K. Jiao-Xun. The numerical stability of linear multistep methods for delay differential equations with many delays. *SIAM J. Numer. Anal.*, 33(3):883–889, 1996.
- [23] Y. Kuang and H. L. Smith. Slowly oscillating periodic solutions of autonomous state-dependent delay equations. *Nonlinear Anal.*, 19(9):855–872, 1992.
- [24] T. Luzyanina and D. Roose. Numerical stability analysis and computation of Hopf bifurcation points for delay differential equations. *J. Comput. Appl. Math.*, 72:379–392, 1996.
- [25] J. M. Mahaffy, J. Bélair, and M. C. Mackey. Hematopoietic model with moving boundary condition and state dependent delay: applications in erythropoiesis. *J. Theor. Biol.*, 190:135–146, 1998.
- [26] J. Mallet-Paret and R. D. Nussbaum. Boundary layer phenomena for differential-delay equations with state-dependent time lags, 1. *Arch. Rational Mech. Anal.*, 120:99–146, 1992.
- [27] J. Mallet-Paret, R. D. Nussbaum, and P. Paraskevopoulos. Periodic solutions for functional differential equations with multiple state-dependent time lags. *Topological Methods in Nonlinear Analysis, J. of the Juliusz Schauder Center*, 3:101–162, 1994.

- [28] J. A. J. Metz and O. Diekmann. *The dynamics of physiologically structured populations*, volume 68 of *Lect. Notes in Biomath.* Springer-Verlag, 1986.
- [29] K. W. Neves and A. Feldstein. Characterization of jump discontinuities for state dependent delay differential equations. *J. Math. Anal. Appl.*, 56:689–707, 1976.
- [30] C. A. H. Paul. A user-guide to Archi - an explicit Runge-Kutta code for solving delay and neutral differential equations. Technical Report 283, The University of Manchester, Manchester Center for Computational Mathematics, December 1997.
- [31] H. L. Smith. Reduction of structured population models to threshold-type delay equations and functional differential equations: a case study. *Math. Biosci.*, 113:1–23, 1993.
- [32] H. L. Smith and Y. Kuang. Periodic solutions of differential delay equations with threshold-type delays. *Contemp. Math.*, 129:153–176, 1992.
- [33] D. R. Willé and C. T. H. Baker. The tracking of derivative discontinuities in systems of delay differential equations. *Appl. Num. Math.*, 9:209–222, 1992.
- [34] M. Yebdri. Special slowly oscillating periodic solution of a state dependent delay differential equation. Report, Institut de Mathématiques, Université de Tlemcen, Tlemcen, Algeria, 1999.